

Effect of Thiazole Derivatives on the Corrosion of Mild Steel in 1 M HCl Solution

Nada Abdulwali^{1,*}, Faez Mohammed¹, Abdosalam Al subari², Hicham Ghaddar³,
Abdallah Guenbour¹, Abdelkbir Bellaouchou¹, El Mokhtar Essassi³, Robert A Cottis⁴

¹ Laboratoire des Matériaux Nanotechnologie et Environnement, Université Mohamed V Agdal.
Faculté des Sciences. Av. Ibn Battouta. BP 1014, Rabat. Maroc.

² Yemeni Jordanian University, sana'a, yemen.

³ Laboratoire de Chimie Organique Hétérocyclique, Université Mohamed V Agdal. Faculté des
Sciences. Av. Ibn Battouta. BP 1014, Rabat. Maroc.

⁴ Corrosion and Protection Centre, School of Materials, University of Manchester, Manchester M13
9PL, UK

*E-mail: nada_alwajih@hotmail.fr

Received: 2 June 2014 / Accepted: 19 July 2014 / Published: 25 August 2014

Corrosion inhibition of carbon steel in normal hydrochloric acid solution at 303 K by new thiazole derivatives has been studied by a series of known techniques such as weight loss, polarisation and electrochemical impedance spectroscopy (EIS). The experimental results have showed that this organic compound revealed a good corrosion inhibition and that the inhibition efficiency is increased with the inhibitor concentration. Potentiodynamic polarisation suggested that it is a mixed type of inhibitor. Impedance measurements showed that the double-layer capacitance decreased and charge-transfer resistance increased with increase in the inhibitors concentration and hence increasing in inhibition efficiency. The adsorption of thiazole on the carbon steel surface, in 1 M HCl solution, obeyed to the Langmuir isotherm with a very high negative value of the standard Gibbs free energy of adsorption $\Delta G^\circ_{\text{ads}}$ (chemisorption).

Keywords: Thiazole derivatives; Corrosion; Inhibition; Mild Steel; Hydrochloric acid.

1. INTRODUCTION

Acid solutions are commonly used for the removal of undesirable scale and rust in the metal working, cleaning of boilers and heat exchangers. Hydrochloric acids are most widely used for all these purposes. However, the strong corrosivity of hydrochloric acid needs to be controlled by an appropriate

corrosion inhibitor [1-4]. The existing data show that most organic inhibitors act by adsorption on the metal surface. The adsorption of inhibitors occurs through heteroatoms such as nitrogen, oxygen, phosphorus and sulphur, triple bonds or aromatic rings. These compounds are adsorbed on the metallic surface block the active corrosion sites. The molecules that, at the same time, contain nitrogen and sulfur in their structures are of particular importance inhibitors. The reason is that these molecules provide excellent inhibition compared with compounds that contain only sulfur or nitrogen [5–8]. In literature many thiazole derivatives have been studied as corrosion inhibitors and found that thiazole derivatives have good corrosion inhibition effect [9–10]. The inhibition property of thiazole compounds is attributed to their molecular structure. The planarity and pairs of free electrons in heteroatoms are important characteristics that determine the adsorption of these molecules on the metal surface. Thiazole derivatives are considered as non-cytotoxic substances. This environmentally friendly property makes them favorable to be used in practice, replacing some toxic organic inhibitors in agreement with the new environmental restrictions need to use green ones [11-12]. On the other hand, the inhibiting efficiency of organic compounds is strongly dependent on the structure and chemical properties of the layer adsorbed on the metal surface. The strength of adsorbed layer is related to the functional groups connected to aromatic ring [13]. The adsorption of organic compounds depends mainly on the electronic structure of the molecule and that the inhibition efficiency increases with the increase in the number of aromatic ring [14-15]. These compounds are adsorbed on the metallic surface and block the active corrosion sites. Adsorption behavior of organic molecules on the surface of metals depends on molecular structure of the organic compounds, surface charge density and zero charge potential of metals [16]. The aim of this work is to investigate the inhibiting influence of thiazole derivatives on mild steel corrosion in 1.0M hydrochloric acid solution. This has been studied by weight loss, potentiodynamic polarization and electrochemical impedance spectroscopy (EIS) techniques.

2. EXPERIMENTAL

2.1. Materials

Mild steel strips with the composition C (0.2%), Mn (0.54%), P (0.16%), S(0.24%), Cr (0.37%), Si (0.53%) and the remainder is Fe and size of (2cm × 1cm × 0.2 cm) were used for weight loss measurements. The mild steel specimens have a rectangular form (length = 0.3 cm, width = 1.1 cm, thickness = 0.2 cm) connected with Cu-wire for electrical conductance used for potentiodynamic polarization and impedance measurements. The electrode was polished using a sequence of emery papers of different grades and then degreased with acetone.

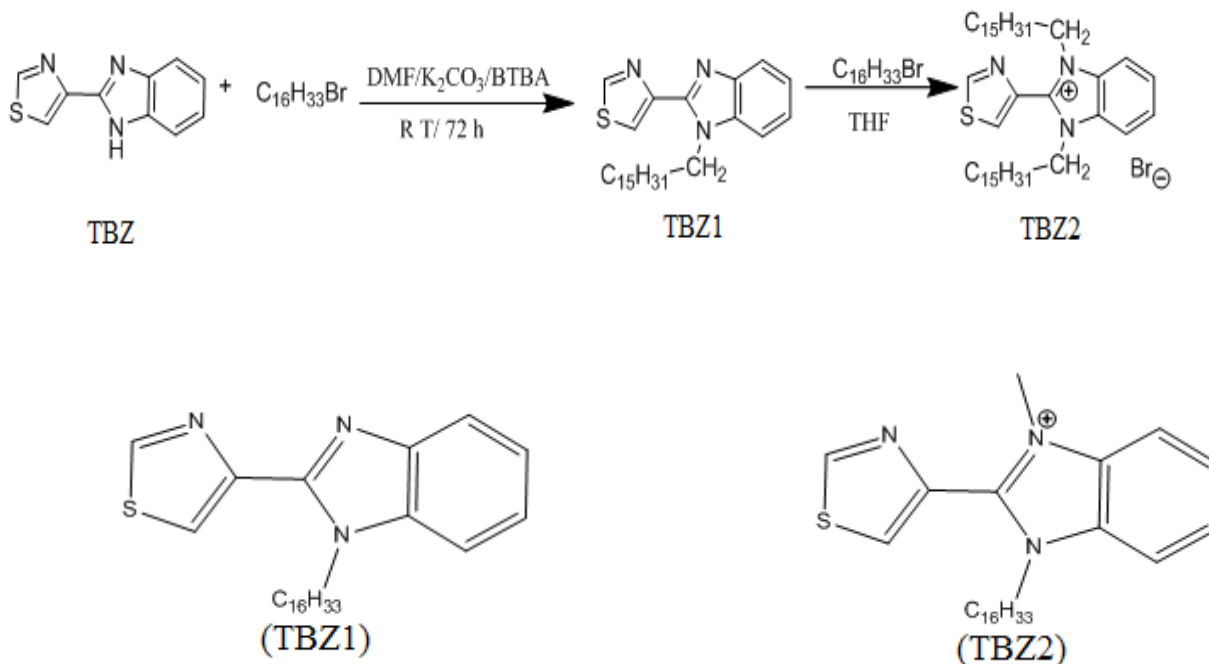
2.2. Inhibitor

2.2.1. Synthesis of inhibitors

The 4-(1-hexadecyl-1H-benzo[d]imidazol-2-yl)thiazole (TBZ1) was synthesized as follows: In a three-neck round bottom flask equipped with condenser, 6 g (29.85mmol) of , 4-(1H-benzo[d]imidazol-2-yl)thiazole(TBZ), was dissolved in 100 ml dimethylformamide (DMF), 6,26 g

(44.8mmol) of potassium carbonate, 24.68 mmol of 1-bromohexadecane and tetra-n-butylammonium bromide (0.1 mmol) were added. The mixture was stirred at room temperature for 72 h. The white solid formed was filtered off and the solvent was evaporated under vacuum and the remaining foam was dissolved in CH₂Cl₂ and filtered. The CH₂Cl₂ was removed and the residue was recrystallized in ethanol to offer the pure product.

In the second step, 20 mmol of The 4-(1-hexadecyl-1H-benzo[d]imidazol-2-yl)thiazole (TBZ1) was dissolved in 50 ml tetrahydrofuran (THF) and 30 mmol of 1-bromohexadecane was added. After 3 h of heating the solvent was removed, the solid product 1,3-dihexadecyl-2-(thiazol-4-yl)-1H-benzo[d]imidazol-3-ium bromide(TBZ2) was recrystallized from ethanol. The structures of the products (TBZ1) and(TBZ2) were established by spectroscopic methods. The synthesis and structures of thiazole derivatives is shown as follows.



(1-hexadecyl-1H-benzo[d]imidazol-2-yl)thiazole (TBZ1)

Yield: 80%. ¹H NMR (CDCl₃): δ(ppm) 9.11, 8.13 (s, 2CH, thiazole); 4.04 (t, 2H, NCH₂, 3J= 7.5 Hz); 1.74 (pent, 2H, NCH₂CH₂, 4J= 7.5 Hz); 1.26 (m, 26H,CH₂); 0.88 (t, 3H,CH₃, 3J= 7.5 Hz); 7.22-7.59 (m, 4H, HAr). ¹³C NMR (CDCl₃): δ 152.5, 120.1(2CH, thiazole); 49.7(NCH₂); 29.9 (NCH₂CH₂); 119.5, 110.1, 123.6, 142.7, 134.2(CHAR); 29.6 (12CH₂); 22.7 , 14.1 (CH₂CH₃). m/z: 425,29 (100,0%), 426,29 (29,4%), 427,28 (4,5%), 427,29 (4,3%), 428,29 (1,4%), 426,28 (1,1%). Elemental Analysis: C, 73.36; H, 9.23; N, 9.87; S, 7.53

1,3-dihexadecyl-2-(thiazol-4-yl)-1H-benzo[d]imidazol-3-ium bromide(TBZ2)

Yield: 60%. ¹H NMR (CDCl₃): δ(ppm) 9.10, 8.13 (s, 2CH, thiazole); 4.04 (t, 4H, NCH₂, 3J= 7.5 Hz); 1.95 (pent, 4H, NCH₂CH₂, 4J= 7.5 Hz); 1.24 (m, 52H,CH₂); 0.89 (t, 6H,CH₃, 3J= 7.5 Hz); 7.22-7.59 (m, 4H, HAr). ¹³C NMR (CDCl₃): δ 152.5, 120.1(2CH, thiazole); 49.7(NCH₂); 29.8 (NCH₂CH₂);

119.5, 110.1, 123.6, 142.7, 134.2(CHAR); 29.6 (12CH2); 22.7 , 14.1 (CH2CH3). m/z: 731,46 (100,0%), 729,46 (97,7%), 732,46 (47,1%), 730,47 (45,2%), 731,47 (10,6%), 733,47 (10,4%), 733,46 (5,2%), 732,47 (2,4%), 734,46 (2,1%), 730,46 (1,9%), 734,47 (1,6%). Elemental Analysis: C, 69.01; H, 9.93; Br, 10.93; N, 5.75; S, 4.39

2.3. Solutions

The aggressive solutions of 1 M HCl were prepared by dilution of analytical grade 37% HCl with doubly distilled water. The concentration range of the inhibitors employed was 1×10^{-5} to 1×10^{-3} M, and the solution in the absence of inhibitors was taken as blank for comparison.

2.4. Weight loss measurements

The gravimetric experiments were carried out in a glass vessel containing 50 mL of 1M HCl with and without the addition of different concentrations (10^{-5} to 10^{-3}) of TBZ1 and TBZ2. Mild steel specimens were immersed in the test acid solutions for 24 h. The glass vessel was inserted into a water bath maintained at 303 K. After the required immersion time, the specimens were withdrawn, rinsed with doubly-distilled water, and then ethanol, and finally dried at room temperature. Then, the loss in weight was determined by analytic balance. The experiments were done in triplicate and the average value of the weight loss was considered. Corrosion rates were calculated from the weight loss of the specimens according to Eq. 1

$$W = \frac{m_1 - m_2}{At} \quad (1)$$

Where m_1 and m_2 are the weight loses (g) before and after immersion in the test solutions, A is the area of the specimens (cm^2), and t is the exposure time (h). The inhibition efficiency (IE) and the degree of surface coverage (Θ) were calculated using the following equations:

$$\text{IE\%} = \left(\frac{W - W'}{W} \right) \times 100 \quad (2)$$

$$\theta = \frac{W - W'}{W} \quad (3)$$

Where W , W' are the uninhibited and inhibited corrosion rates (in terms of $\text{g cm}^{-2} \text{ h}^{-1}$), respectively.

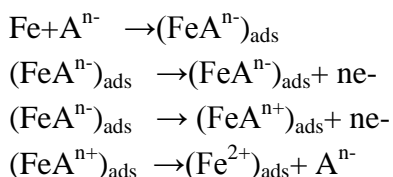
2.5. Potentiodynamic polarization measurements

Before each polarization experiment, the working electrode was first immersed into the test solution for 30 min at (303 K) in order to attain its free corrosion potential, which was recorded as a function of time. After this time a steady-state, corresponding to the corrosion potential (E_{corr}) of the

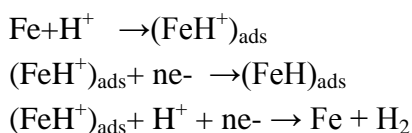
working electrode, was obtained. The electrochemical experiments were carried out in a conventional three electrode electrochemical cell with a platinum counter electrode and saturated calomel electrode (SCE) as reference electrode. The scan rate of potential was 1.0 mV s^{-1} and the potential was scanned in the range of -900 mV/SCE to -250 mV/SCE . Polarization data were recorded using a digital potentiostat model Volta lab PGZ301 driven by Volta Master soft-ware. The polarization curves were carried out in the absence and presence of different concentrations of inhibitors. The IE (%) was calculated from:

$$\text{IE\%} = \left(\frac{I_{\text{corr}} - I'_{\text{corr}}}{I_{\text{corr}}} \right) \times 100 \quad (4)$$

Where I_{corr} and I'_{corr} are the uninhibited and inhibited corrosion current densities respectively. Some of the authors proposed the following mechanism for the corrosion of mild steel in acid solution [17-19]:



The cathodic hydrogen evolution



The electrochemical impedance spectroscopy (EIS) measurements were carried out at the open circuit potential (E_{ocp}), using a computer-controlled potentiostat (Voltalab). Impedance spectra were obtained in the frequency range of 100 kHz to 100 mHz after 30min of immersion in the test solutions. A sine wave with 10 mV amplitude was used to perturb the system. The impedance diagrams are given in the Nyquist representation.

2.6. Free energy of adsorption

$\Delta G_{\text{ads}} = -RT \ln (K / 55.5) \text{ KJ/mole}$, where ΔG_{ads} = free energy of adsorption; R = Gas Constant in KJ; T = Temperature in K; K = Adsorptive equilibrium constant; and the value of 55.5 is the concentration of water in solution expressed in L^{-1} mol.

From the above equation, the free energy change of adsorption in all the various concentrations of TBZ at (303K) of temperature and 10^{-3}M concentration (best inhibition) of TBZ were calculated.

2.7. SEM analysis

The surface morphology of the mild steel samples after 3h of immersion in 1M HCl solution with and without inhibitor, were investigated by scanning electron microscope (SEM) using a Quanta 200 FEG model No.D7860 (XTM @ 2001 FEI Company).

3. RESULTS AND DISCUSSION

3.1. Weight loss measurements

The corrosion parameters such as inhibition efficiency, IE (%) and corrosion rate ($\text{g cm}^{-2} \text{ h}^{-1}$) at different concentration of TBZ1 and TBZ2 in 1M HCl at 303K are presented in Table 1. The results show that the IE increases and the corrosion rate decreases with increase in inhibitor concentration. The IE data showed that TBZ2 has greater interaction with mild steel compared to TBZ1. However, the difference between efficiencies was low and indicated that both compounds exhibit good effectiveness. This may be interpreted by the presence of six double bonds near three nitrogen atoms and one sulphur atom in the structure of both inhibitors. The presence of this kind of cyclic rings and the heteroatoms facilitates the adsorption process. The efficiency passed from 94,5% to 95,3% at TBZ1 and TBZ2 at 10^{-3}M , respectively as shown in Fig. (1, 2).

Table 1. Gravimetric results of Mild steel in 1M HCl at different concentration of each inhibitor at 24h and 303 K.

Inhibitors	Conc(M)	Wcorr(g/cm ² .h)	IE(%)	Θ
HCl 1M	0	0.445	-	
TBZ1	1.10^{-5}	0.0662	85,1	0,851
	5.10^{-5}	0.0560	87,4	0,874
	1.10^{-4}	0.0422	90,5	0,905
	5.10^{-4}	0,0337	92,4	0,924
	1.10^{-3}	0,0242	94,5	0,945
TBZ2	1.10^{-5}	0.0359	91,9	0,919
	5.10^{-5}	0,0306	93,1	0,931
	1.10^{-4}	0,0274	93,8	0,938
	5.10^{-4}	0,0254	94,3	0,943
	1.10^{-3}	0,0210	95,3	0,953

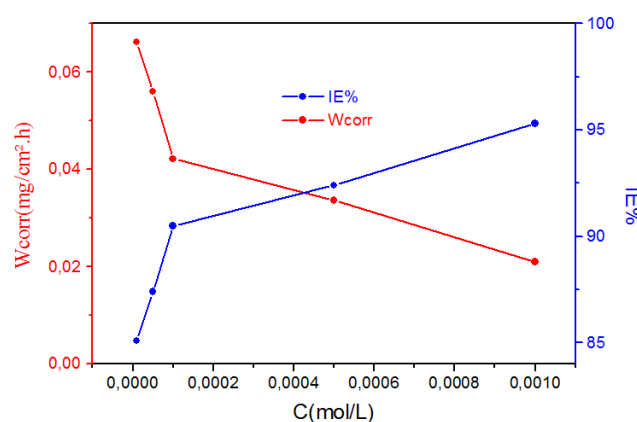


Figure 1. Variation of inhibition efficiency and corrosion rate in 1M HCl on steel surface without and with different concentrations of TBZ2.

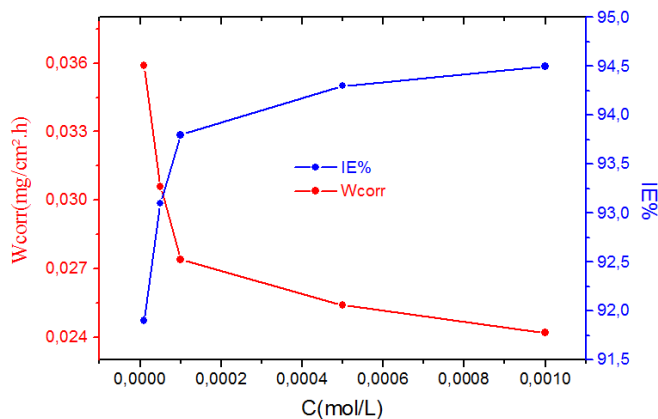


Figure 2. Variation of inhibition efficiency and corrosion rate in 1M HCl on steel surface without and with different concentrations of TBZ1.

3.2. Tafel polarization measurements

Figures 3 and 4 show potentiodynamic curves for the mild steel electrode in 1M HCl solution with and without different concentrations of inhibitors TBZ1 and TBZ2. It is clear that the current density decreases with the presence of Inhibitors; this indicates that these compounds are adsorbed on the metal surface and hence inhibition occurs. Values of corrosion potential (E_{corr}), corrosion current density (I_{corr}), obtained by extrapolation of the Tafel lines, cathodic, and anodic Tafel slope ($-bc$, ba), and corrosion IE (%) for different concentrations of inhibitors TBZ1 and TBZ2 in 1M HCl are given in Table 2.

Table 2. Polarization parameters and the corresponding inhibition efficiency for the corrosion of mild steel in 1 M HCl containing different concentrations of thiazole derivatives at 303K.

Inhibitors	C_{inh}	E_{corr} (mV/ECS)	I_{corr} (μ A/cm 2)	$-bc$ (mV/dec)	ba (mV/dec)	E%
HCl 1M	0	-338	849	285	74	----
TBZ1	10^{-5}	-422	159	175	62	81.3
	5.10^{-5}	-430	156	176	59	81.6
	10^{-4}	-420	82	254	74	90 .3
	5.10^{-4}	-448	75	256	86	91.2
	10^{-3}	-443	52	266	86	94 .0
TBZ2	10^{-5}	-429	106	320	102	87.5
	5.10^{-5}	-446	104	310	110	87.8
	10^{-4}	-429	87	312	100	89.8
	5.10^{-4}	-453	81	389	106	90.5
	10^{-3}	-447	60	356	92	92.9

The potentiodynamic curves show that there is a clear reduction of the cathodic currents in the presence of both inhibitors compared with the blank solution. It is clear that the cathodic reaction

(hydrogen evolution) was inhibited. The values of cathodic Tafel slope (bc) for two thiazole compounds are found to increase in the presence of inhibitor. The Tafel slope variations suggest that both thiazole compounds influence the kinetics of the hydrogen evolution reaction [20]. This indicates an increase in the energy barrier for proton discharge, leading to less gas evolution [21]. The approximately constant values of anodic Tafel slope (ba) for both thiazole compounds indicate that these compounds were first adsorbed onto the metal surface and impeded by merely blocking the reaction sites of the metal surface without affecting the anodic reaction mechanism [22]. It can be seen from Table 2 that the corrosion potentials of both inhibitors shift in the negative direction. The shift of the corrosion potential in the negative sense as compared to the uninhibited situations shows that the effect on the cathodic branch and reaction is somewhat more pronounced than on the anodic reaction. The compounds tested as corrosion inhibition of mild steel in 1M HCl are effective even with small concentrations. The higher values of IE indicate the higher surface coverage, due to the inhibitors adsorption on the metal surface.

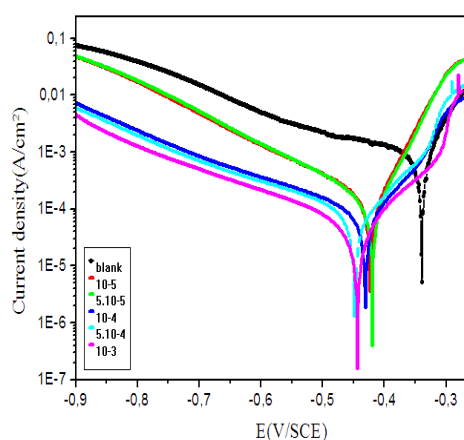


Figure 3. Polarization curves for mild steel in 1 M HCl containing different concentrations of TBZ2.

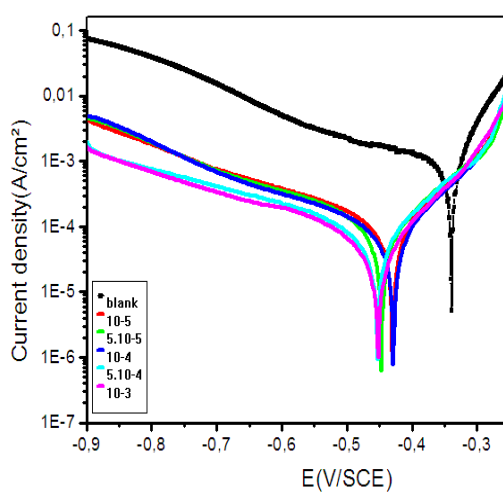


Figure 4. Polarization curves for mild steel in 1 M HCl containing different concentrations of TBZ1.

3.3. Electrochemical impedance spectroscopic studies

Impedance measurement has been widely used in investigating corrosion inhibition processes. It provides information on both the resistive and capacitive behaviour at interface and makes it possible to evaluate the performance of the tested compounds as possible inhibitors against metallic corrosion.

The corrosion behaviour of mild steel in 1 M HCl in the presence of thiazole derivatives was investigated by EIS at 303 K after 30 min of immersion. The Nyquist plots of mild steel in inhibited and uninhibited acidic solutions containing various concentrations of inhibitors are shown in Figs(5,6) After analyzing the shape of the Nyquist plots, it is concluded that the curves approximated by a single capacitive semi-circles, showing that the corrosion process was mainly charge transfer controlled [23]. The general shape of the curves is very similar for all samples; the shape is maintained throughout the whole concentrations, indicating that almost no change in the corrosion mechanism occurred due to the inhibitor addition [24]. The diameter of Nyquist plots (R_{ct}) increases on increasing the inhibitors concentration. These results suggest the inhibition behaviour of thiazole derivatives on corrosion of mild steel in 1 M HCl solution.

The impedance parameters including charge transfer resistance R_{ct} , double layer capacitance C_{dl} and inhibition efficiency IE% is given in Table 3. Charge transfer resistance R_{ct} increases from 42.00 to 600 and 496 $\Omega \cdot \text{cm}^2$ for TBZ1and TBZ2 respectivement and double layer capacitance C_{dl} decreases from 94 .22 to 27.80 and 32.29 $\mu\text{F}/\text{cm}^2$ for TBZ1and TBZ2 respectivement with the increase of thiazole derivatives concentration. The decrease in C_{dl} means that the adsorption of inhibitor takes place on the mild steel surface in acidic solution. C_{dl} values were calculated from the frequency at which the imaginary component of impedance was maximum ($Z_{im\ max}$) using the relation:

$$C_{dl} = \frac{1}{2\pi f_{max} R_{ct}} \quad (5)$$

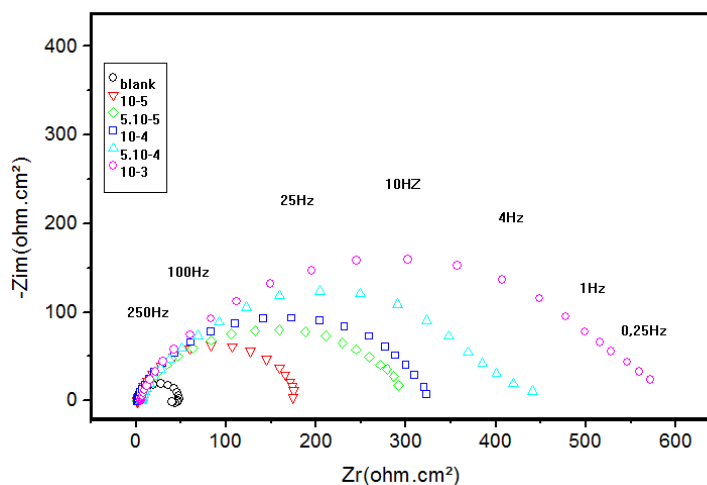
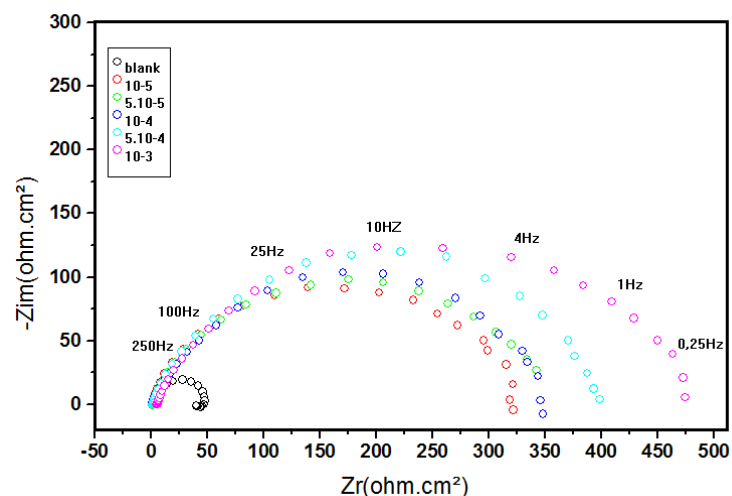
Where f_{max} is the frequency at which the imaginary component of impedance is maximum. The inhibition efficiency got from the charge-transfer resistance is calculated by the following relation:

$$\text{IE}(R)\% = \frac{R_{ct} - R^{\circ ct}}{R_{ct}} \times 100 \quad (6)$$

Where R_{ct} and $R^{\circ ct}$ represent the resistance of charge transfer in the presence and absence of inhibitor, respectively. R_{ct} is the diameter of the loop. The increase in the resistance of charge transfer leads to an increase of inhibition efficiency. The results indicate good agreement between the values of inhibition efficiency as obtained from the impedance technique and polarization measurements. It is concluded that the corrosion rate depends on the chemical nature of the electrolyte rather than the applied technique [25].

Table 3. Corrosion parameters obtained by impedance measurements for mild steel in 1 M HCl at various concentrations of thiazole derivatives at 303K.

Inhibitors	C inh(M)	Rs	Rct	Cdl($\mu\text{F}/\text{cm}^2$)	IE(R)%
TBZ1	1M	1.4	042	94.22	-
	10^{-5}	1.7	249	63.79	83.1
	5.10^{-5}	1.4	304	82.79	86.2
	10^{-4}	1.4	324	77.38	87.0
	5.10^{-4}	1.6	425	42.80	90.1
	10^{-3}	1.8	600	27.80	93.0
TBZ2	10^{-5}	1.2	322	48.54	86.9
	5.10^{-5}	1.5	359	30.43	88.3
	10^{-4}	1.0	363	45.25	88.4
	5.10^{-4}	1.6	420	62.59	90.0
	10^{-3}	1.2	496	32.29	91.5

**Figure 5.** Nyquist plots for mild steel in 1 M HCl without and with different concentrations of TBZ1**Figure 6.** Nyquist plots for mild steel in 1 M HCl without and with different concentrations of TBZ2

3.4. Free Energy of Adsorption (ΔG_{ads})

The nature of corrosion inhibition is deduced through the adsorption characteristics of the inhibitor. The metal surface in aqueous solution is always covered with adsorbed water dipoles. Therefore, the adsorption of inhibitor molecules from aqueous solution is a quasi substitution process [26]. Surface coverage degrees (Θ) for various concentrations of thiazole derivatives in 1 M HCl have been evaluated from inhibition efficiency values. These values were collected from Weight loss measurements. In order to evaluate the adsorption process of inhibitor on the mild steel surface, many of adsorption isotherms were tested. The best fit between the experimental results and the isotherm function was found in Langmuir adsorption isotherm which is expressed as Eq. (7) [27]:

$$\frac{Cinh}{\Theta} = \frac{1}{K_{ads}} + Cinh \quad (7)$$

Where $Cinh$ is inhibitor concentration, Θ is the degree of coverage on the metal surface and K_{ads} is the equilibrium constant for adsorption process.

To calculate the surface coverage; Θ , it was assumed that the inhibitor efficiency is due mainly to the blocking effect of the adsorbed species and hence $IE (\%) = 100 \times \Theta$ [28].

The value of K is related to the standard free energy of adsorption, ΔG_{ads} , by the following equation [29]:

$$\Delta G_{ads}^0 = -RT \ln(55.5K_{ads}) \quad (8)$$

Where R is the gas constant and T is the absolute temperature. The value of 55.5 is the molar concentration of water in solution expressed in mol l⁻¹.

The values of adsorption constant, slope, and linear correlation coefficient (R^2) can be obtained from the regressions between C/Θ and C(fig7), and the results are listed in Table 4. The result shows that all the linear correlation coefficients and all the slopes are close to one and confirm that the adsorption of thiazol derivatives in 1 M HCl follows the Langmuir adsorption isotherm. The thermodynamic parameters for adsorption process obtained from Langmuir adsorption isotherms for the studied thiazol derivatives are given in Table 4. The negative values of ΔG_{ads} and the higher values of K_{ads} reveal the spontaneity of adsorption process and they are characteristic of strong interaction and stability of the adsorbed layer with the steel surface.

Table 4. Thermodynamic parameters for the adsorption of thizole derivatives in 1 M HCl on the mild steel at 303K.

inhibitors	R^2	K_{ads}	ΔG_{ads}^0 (kJ/mol)
TBZ1	0.9997	91170.2	- 38.2
TBZ2	0.9995	361833.8	- 41.6

It generally accepted that the values of ΔG° ads up to -20 kJ mol⁻¹, the types of adsorption were regarded as physisorption, the inhibition acts due to the electrostatic interactions between the charged

molecules and the charged metal, while the values around -40 kJ mol^{-1} or smaller(more negative), were seen as chemisorptions, which is due to the charge sharing or a transfer from the inhibitor molecules to the metal surface to form a covalent bond [30, 31]. The values of $\Delta G^\circ \text{ ads}$ in our measurements range from $-41,6$ to $-38,2 \text{ kJ mol}^{-1}$ (in Table 4), it is suggested that the adsorption of these thiazole derivatives involve chemisorptions of interaction.

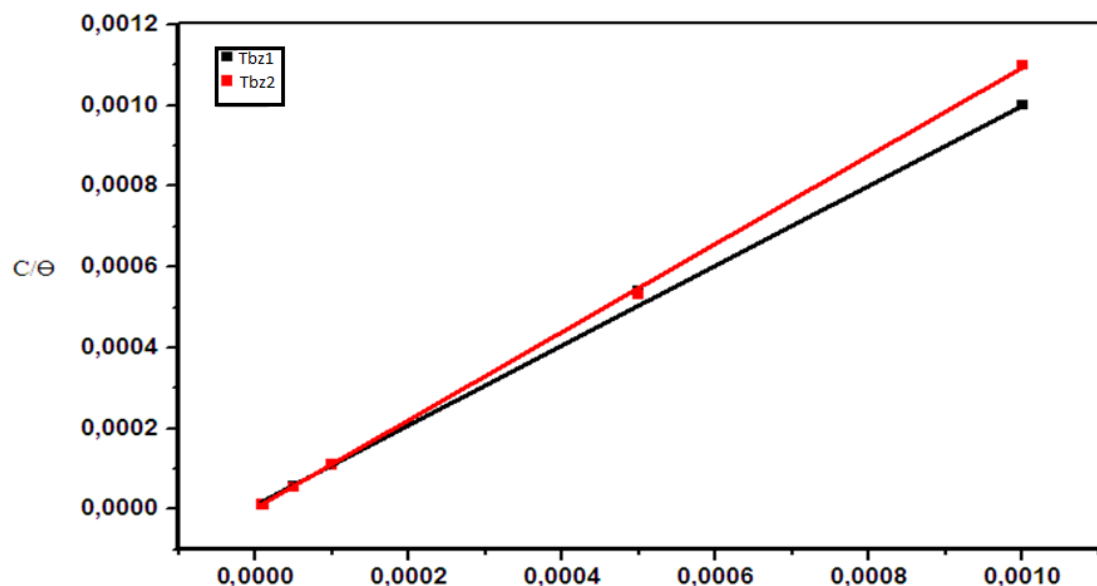
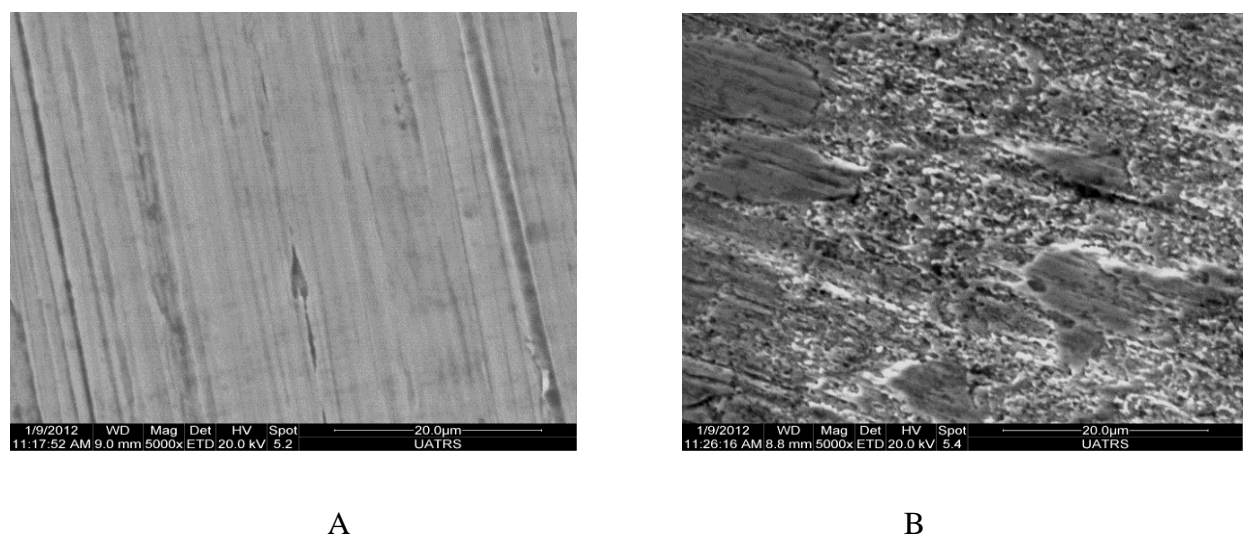


Figure 7. Langmuir isotherm adsorption of thiazole derivatives on the surface of mild steel in 1 M HCl at 303K.

3.5. Scanning electron microscopy

In order to evaluate the conditions of the steel surfaces in contact with hydrochloric acid solution, samples were imaged in the SEM.



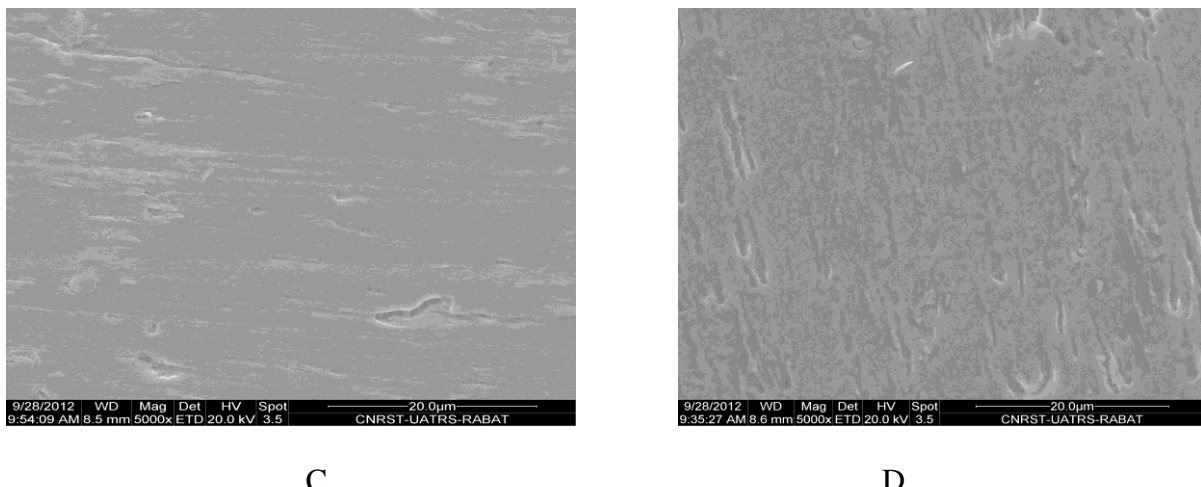


Figure 8. SEM micrographs of mild steel samples at 303 K (a) only surface polishing, (b) after immersion in 1 M HCl without inhibitor, (c) after immersion in 1 M HCl in presence of 1.0×10^{-3} M TBZ1 and (d) after immersion in 1 M HCl in presence of 1.0×10^{-3} M TBZ2.

Surface was observed before and after 24 h of immersion in 1 M HCl in the absence and presence of inhibitor at 303 K. Fig.8(a)shows the polished surface of steel before being exposed to the testing environment. The polishing lines of the steel surface are visible in Fig.8 (a). Fig8(b)shows the SEM image surface of steel after immersion in 1 M HCl, this reveals a severe damage on surface due to metal dissolution. Fig.8(c) and Fig.8(d) show the steel surface protected after adding 10^{-3} M of inhibitors, it is observed that the surface damage has diminished in comparison to the blank material.

4. CONCLUSION

The following results can be highlighted from this study.

(1) The corrosion rates of the mild steel decrease as the concentration of TBZ derivatives increases. The inhibition efficiency increases with the increase of inhibitor concentration and the maximum inhibition efficiency is approximately 95% in 10^{-3} M of TBZ2.

(2) The TBZ derivatives acts as a mixed inhibitor for corrosion of mild steel in 1M HCl retarding the anodic and cathodic corrosion reactions with predominant effect on the cathodic reaction.

(3) EIS results indicate that as the additive concentration was increased the resistance of charge transfer increased whereas double-layer capacitance decreased.

(4) The adsorption of TBZ derivatives on the mild steel surface in 1M hydrochloric acid obeys a Langmuir adsorption isotherm. The negative value of obtained from the study indicates that TBZ derivatives was strongly adsorbed on the steel surface and predominantly by chemisorption.

(5) The SEM micrographs of the mild steel corrosion in 1M HCl solution confirm the protection by the Thiazole derivatives studied.

References

1. F. Bentiss, M. Bouanis, B. Mernari, M. Traisnel, H. Vezin, M. Lagrenée, *Appl. Surf. Sci.* 253 (2007) 3696–3704 (and references therein).
2. M.A. Amin, S.S. Abd El-Rehim, E.E.F. El-Sherbini, R.S. Bayyomi, *Electrochim. Acta* 52 (2007) 3588.
3. P. Bommersbach, C. Alemany-Dumont, J.P. Millet, B. Normand, *Electrochim. Acta* 51 (2005) 1076–1084.
4. M.A. Quraishi, J. Rawat, *Mater. Chem. Phys.* 77 (2002) 43–47.
5. H.H. Hassan, E. Abdelghani, M.A. Amin, *Electrochim. Acta* 52 (2007) 6359.
6. H.H. Hassan, *Electrochim. Acta* 53 (2007) 1722.
7. Y. Abboud, A. Abourriche, T. Saffaj, M. Berrada, M. Charrouf, A. Bennamara, N. Al Himidi, H. Hannache, *Mater. Chem. Phys.* 105 (2007) 1.
8. M.A. Quaraishi, J. Rawat, M. Ajmal, *J. Appl. Electrochem.* 30 (2000) 745.
9. M.L. Zheludkevich ,K.A. Yasakau,S.K. Poznyak M.G.S. Ferreira, *Corros. Sci.* 47 (2005) 3368.
10. Gy. Vastag, E. Szocs, A. Shaban, I. Bertoti, K. Popov-Pergal, E. Kalman, *Solid State Ionics* 141 (2001) 87.
11. O.K.Aboia, A.O. James, *Corros. Sci.* 52(2) (2010) 661.
12. N.O.Eddy, S.A.Odoemelam, *Pigment and Resin Technology* 38(2) (2009) 111.
13. A.J. Szyprowski, *Br. Corros. J.* 35(2)(2000)155.
14. S. L. Granese, B. M. Rosales, C. Oviedo, J. O. Zerbino, *Corros.Sci.* 33(1992)1439.
15. M.Abdallah, A.M. El Defrawy,I. A. Zaafarany, M.Sobhi, A.H.M. Elwahy, and M. R. Shaaban, *Int. J. Electrochem. Sci.*, 9 (2014) 2186 – 2207.
16. J.Z. Ai, X.P. Guo, J.E. Qu, Z.Y. Chen, J.S. Zheng, *Colloids Surf. A: Physicochem. Eng.Asp.* 281 (2006) 147.
17. Morad, M.S., El-Dean, A.M.K. *Corros. Sci.* 48 (2006) 3398.
18. Tebbji, K., Hammouti, B., Oudda, H., Ramdani, A., Benkaddour, *M. Appl. Surf. Sci.* 252 (2005) 1378.
19. Yurt, A., Balaban, A., Ustun Kandemir, S., Bereket, G., Erk, *B. Mater. Chem. Phy.* 85 (2004) 420.
20. G. Quartarone, L. Bonaldo, C. Tortato, *Appl Surf Sci .Tortato C.*, 252 (2006) 8251.
21. S. Tamil Selvi, V. Raman, N. Rajendran, *J Appl Electro-chem.* 33 (2003)1175.
22. LR. Chauhan, G. Gunasekaran, *Corros Sci.* 49 (2007) 1143.
23. R. Rosliza, W.B. Wan Nik, H.B. Senin, *Mater. Chem. Phys.* 107 (2008) 281–288.
24. F.M. Reisde, H.G. Melo, I. Costa, *Electrochim. Acta* 51 (2006) 1780–178.
25. M. Abdel-Gaber, B.A. Abd-El-Nabey, I.M. Sidahmed, A.M. El-Zayaday, M. Saadawy, *Corros. Sci.* 48 (2006) 2765–2779.
26. L.R. Chauhan, G. Gunasekaran, *Corros. Sci.* 49 (2007) 1143.
27. R. Solmaz, E. Altunbas, G. Kardas, *Protec. Met. Phys. Chem. Surf.* 47 (2) (2011) 264.
28. P. Li, J.Y. Lin, K.L. Tan, J.Y. Lee, *Electrochim. Acta* 42 (1997) 605.
29. M.Z.A. Rafiquee, N. Saxena, S. Khan, M.A. Quraishi, *Mater. Chem. Phys.* 107 (2008) 528.
30. Z. Szklarska-Smialowska, J. Mankowski, *Corros. Sci.* 18 (1978) 953.
31. A. Yurt, S. Ulutas, H. Dal, *Appl. Surf. Sci.* 253 (2006) 919.